THE FEATURES OF STRESS FIELD IN THE JAVAKHETI VOLCANIC HIGHLAND DETERMINED BY THE EARTHQUAKE FOCAL MECHANISMS FOR THE TIME PERIOD 2005-2017

© 2018   E.E.Sahakyan

Institute of Geological Sciences
National Academy of Sciences Republic of Armenia
24A M. Baghramyan Ave. 0019, Yerevan, Armenia
E-mail: elya.sahakyan@gmail.com
Reclived by the editor 07.05.2018

The Javakheti Volcanic Highland, located in the central Caucasus, is part of the Arabia-Eurasia continental collision zone. This area is characterized by increased seismic activity and volcanism where earthquake distribution is diffuse. In this study, source mechanisms of earthquakes using digital waveform data recorded by seismic stations of the Armenian, Georgian, and adjacent seismic networks have been investigated. The focal mechanisms of a set of earthquakes that occurred within 2005–2017 with high reliability, based on the polarity of the first motion of the P-wave have been constructed. The azimuth, angle of incidence, and polarities of the P-phase were used to obtain initial focal mechanism solutions. A re-location for selected seismic events during this time period was also performed.

The fault plane solutions of the recorded earthquakes were used to determine the actual fault geometry, faulting type, and stress regime of the study area. We combined all of the reliably determined focal mechanisms across the dozens of earthquakes to investigate the current crustal stress status in the Javakheti Volcanic Highland. The solutions of the different mechanisms vary between strike-slip, thrust, and normal, but are mainly thrust for the time period 2005-2017.

The thrust and strike-slip stress regimes are observed in the study area.

INTRODUCTION

According to Zoback, knowing the patterns and variations of a region's stress field is critical for understanding the local and regional effects induced by large-scale plate tectonics and the subsequent deformation field (Zoback, 1980). Along this line of reasoning, the primary goal of this study is to use focal mechanism solutions to investigate the current crustal stress field states and tectonic regime of the Javakheti Volcanic Highland.

The Javakheti Volcanic Highland is characterized by seismic and volcanic activity, where earthquake epicenters are diffusely distributed. In this study we determine focal mechanism solutions for a set of earthquakes that occurred from 2005–2017 based on the polarity of P-wave first motion, using the digital waveform data recorded by the Armenian, Georgian, and adjacent seismic networks. Only earthquakes for which the number of polarities is equal to or greater than 12, and azimuthal gaps are less than 100°, and events with low RMS, have been included in the analysis.

For the calculation of focal mechanisms from first motion polarities, we apply the software package FA2004 of Lander (Lander, 2004). Analysis of earthquakes focal mechanism using inversion methods allows us to determine active stress states; therefore, in this study we used Delvaux and Speerner (2003)'s method, which allows us to determine the best-fit regional principal stress directions (compression, intermediate, and tension) σ1, σ2, and σ3, and the relative magnitudes of the stress axes (R= (σ2–σ3)/(σ1–σ3)). The WinTensor program (Delvaux et al., 2003) was used to determine the orientation and shape of the stress tensor. Stress orientations were found to be the maximum (σ1) and minimum principal stresses (σ3); from this, the region's stress regimes were determined.

BACKGROUND

The Javakheti Volcanic Highland is one of the major seismic hazard zones in the Lesser Caucasus (Balassanian et al., 1999; Duff et al., 1980). The Highland is located in the central Caucasus, and is part of the Arabia-Eurasia continental collision zone. Based on global positioning system (GPS) data, the Highland is characterized by N-S compressional (3.5mm/year) and W-E extensional (3.7mm/year) fields (Davtyan, 2007).

The most important fault system adjacent to Javakheti Highland, is Pambak-Sevan-Syunik fault system (PSSF), represented by a 400±10km long NW-SE right-lateral strike-slip fault (Karakhanyan et al., 2016). The present long-term horizontal slip rate along the fault varies between 0.5 and 3–4mm/yr (Philip et al., 2001), which is consistent with the GPS-measured 0.3–3mm/yr (Reilinger et al., 2006; Karakhanyan et al., 2013). PSSF-1 segment located immediately to the south of Javakheti Highland within Armenia changes direction from NW-SE to W-SW-S direction.

The main fault in the studied area is NW-SE 77 km long Javakheti fault located to the north of the PSSF-1 segment that was jointly studied in 2007–2012 with colleagues from Georgia, the United States, and France (Karakhanyan et al., 2012). The fault is oriented to the N-NW and consists of individual segments with clear left-stepping geometry. Fault kinematics is represented by right-lateral strike slip with a normal-fault component. The fault formed distinct scarps, deforming young volcanic and glacial sediments. The largest displacements recorded in the central part of the fault range up to 150–200m by normal slip and 700–900m right-laterally (Karakhanian et al., 2016).

The study area is characterized by long-lasting Pliocene-Quaternary volcanic activity, clustered mostly within Javakheti, Samsari, and volcanic ridges that represent continuums of volcanic cones extended N-S for 55km, and SW-NE for 35km, accordingly (Lebedev et al., 2003). The youngest manifestation of volcanism has been found in the Samsari Ridge confirmed by K-Ar age determinations (Lebedev, et al., 2003) and recent K-Ar and ^{40}Ar/^{39}Ar dates by Nomade et al., (2015) and correspond to time interval between Middle and Late Pleistocene- Holocene (0.8-0 Ma), (Lebedev et al., 2003) distinguishes four

episodes of magmatic activity – Early Pleistocene (800-700Ka), Early-Middle Pleistocene (~400Ka), Middle Pleistocene (320-170Ka), Late Pleistocene-Holocene (<50Ka) – and suggests that some sectors of the Samsari Ridge are potentially hazardous from the viewpoint of volcanic unrest.

METHODOLOGY AND DATA FOR FOCAL MECHANISM SOLUTIONS

In this study, new focal mechanism solutions are constructed for 58 earthquakes (M ≥ 3.0) that occurred between 2005 and 2017 in the Javakheti Volcanic Highland (Fig. 1). The digital waveform data for these events was extracted from the database of the Armenian and Georgian seismic networks. Additional information from the surrounding regional stations was also extracted as digital waveforms from the database of Incorporated Research Institutions for Seismology (IRIS, Washington, http://ds.iris.edu/ds/).

A re-location for 58 selected seismic events during this same time period (2005-2017) was performed using the HYPO71 Program. Events which fulfilled the following conditions were selected and the conditions are at least very clear more than 12 P-wave phases, good azimuth coverage of stations and keeping only events with low RMS.

For determining fault plane geometry, the first motion polarity technique was applied to the earthquakes (Введенская и др, 1960). The FA2004 software package (Lander, 2004) was used for determining focal mechanisms. This software depends on the azimuth, angle of incidence, and polarities of P-phase. Any P-wave ray path leaving the source can be identified by two parameters: the azimuth from the source, φ, and the angle of incidence, i_0, which is a function of the distance, Δ, between the source and the recording station.

Earthquake focal mechanisms were determined geometrically, from the orientations of the P and T kinematic axes bisecting the angles between the fault plane and the auxiliary plane. They can also be determined by the orientation of one of the two nodal planes and the associated slip vector. From this, focal mechanism solutions are constructed for selected earthquakes with 2 nodal planes (Strike, Dip, Rake parameters, Compressional (P) and Tension (T) kinematic axes).

STRESS TENSOR INVERSION METHOD

The current state of the crustal stress field was determined for the study area.

Using inversion methods to resolve earthquake focal mechanisms allows us to determine the active stress state; therefore, in this study we apply the Delvaux and Speerner method (2003), which allows us to determine the best-fit regional principal stress directions, $\sigma1$, $\sigma2$, and $\sigma3$, and the ratio R= ($\sigma2$-$\sigma1$)/($\sigma3$-$\sigma1$) with F (the average degree of misfit), as well as to estimate the associated uncertainty in the solution (Delvaux et al., 2003). Here $\sigma1$, $\sigma2$, and

σ3 indicate maximum, intermediate and minimum principal compressive stresses, respectively (where σ1≥σ2≥σ3).

The ratio R is a measure of the value of the intermediate principal stress (σ2) relative to the maximum (σ1) and minimum (σ3) stresses, and it thus constrains the shape of the stress ellipsoid. The aforementioned method proposes a grid search method of inverting focal mechanisms to obtain the stress tensor (focal mechanisms stress inversion, WinTENSOR), in which stress field parameters are systematically tested against the focal mechanism orientations, and the calculated misfit depends on the orientations of fault planes and slip directions indicated by earthquake focal mechanisms. The system compares the values of the misfit function for each pair of focal planes in order to separate actual movement planes from the auxiliary plane. This function minimizes the deviation between the observed and theoretical slip directions on the plane, minimizes the normal stress, and maximizes the shear stress magnitude on the plane, in order to favor the slip on that plane. WinTensor software allows also determining the direction of maximum and minimum horizontal stresses (SHmax and SHmin).

According to the direction of the compressional and tensional kinematic axis, 3 distinct regions were defined in the study area. Stress regimes were determined for these defined regions.

The stress regime can be expressed numerically by the stress regime index (R'), defined in Delvaux et al. (1997b). The main stress regime is a function of the orientation of the principal stress axes and the shape of the stress ellipsoid: extensional, strike-slip and compressional. For each of these three regimes, the value of the stress ratio R fluctuates between 0 and 1. When the value is close to 0.5 (plane stress), the stress regimes are said to be 'pure' extensional/strike-slip/compressional.

RESULTS AND DISCUSSION

The fault plane solutions of the 58 recorded earthquakes (M≥3.0) (fig.1) were used to determine the type of faulting and the stress regime of the Javakheti Volcanic Highland.

The analyzed earthquakes have a variety of focal mechanisms, and the fault planes of those events have different compression and dilatation distributions. Analysis of focal mechanism distribution indicates that the stress status of the crust varies across the study area.

The focal mechanism solutions of these events demonstrate the present-day tectonic activity in this area. The distributions of the different mechanisms vary between strike-slip, normal, and thrust, but are mainly thrust (fig.1). 16 events give pure normal faults and normal faults with minor strike-slip component, with the fault planes trending NE-SW. These events primarily occurred in the north-eastern part of the study area, concentrated within the territory of Javakheti ridge.
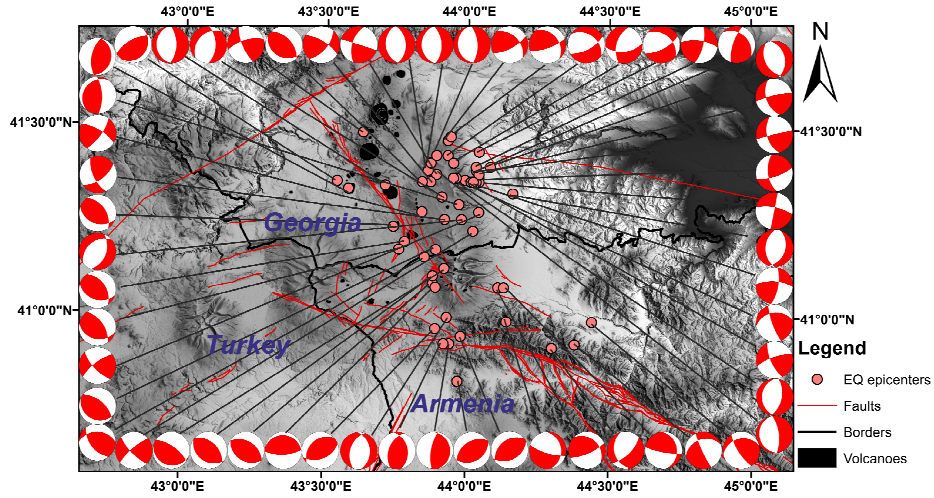
Figure 1. Fault plane solutions of the selected 58 earthquakes that occurred in the study area between 2005 and 2017, with M ≥ 3.0

26 events are characterized by thrust fault mechanisms, which are related to the active faulting in the study area. The P compression axes coincide with the general compression direction of the Caucasus region (trending from NE to SW). 16 events are associated with strike-slip (SS) faults, trending primarily N-S.

Distribution of types of mechanisms can be seen in dip angles based ternary diagram (fig.2).
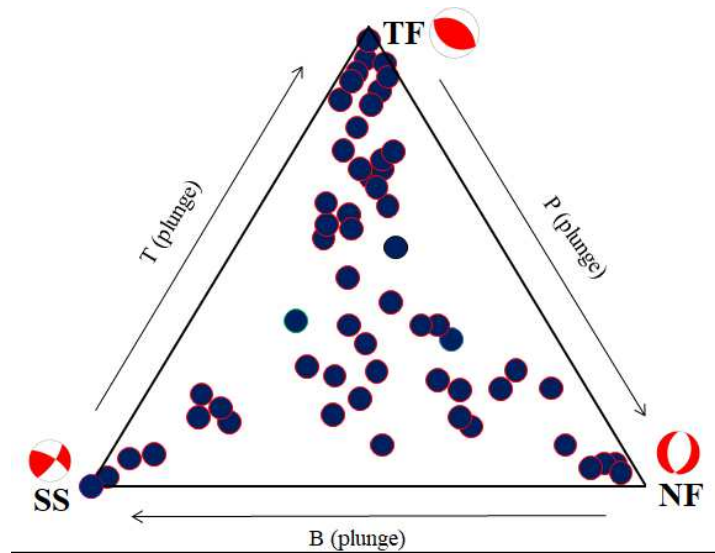
Figure 2. Ternary diagram of 58 earthquakes that occurred in the study area between 2005-2017

Triangle diagrams are simply a quantitative graphical method for using the dip angles of T, B and P axes (δ_T, δ_B and δ_P) for displaying focal mechanisms.

It is possible to plot a unique point representing the orientation of the T, B, and P axes because any three mutually perpendicular vectors having dip angles δ_T, δ_B and δ_P satisfy the identity

$$sin^2\delta_T + sin^2\delta_B + sin^2\delta_P = 1$$

If we define x= sin δ_T, y= sin δ_B, and z= sin δ_P, this identity is just the equation of the sphere $x^2+y^2+z^2=1$. Since all the angles are between 0 and 90 °, at the vertices of the triangle the dip angles are 90^0. The vertices of the triangle represent earthquakes with vertical T axes (thrust mechanisms), vertical B axes (strike slip), and vertical P axes (normal) (Froehlich C., 1992).
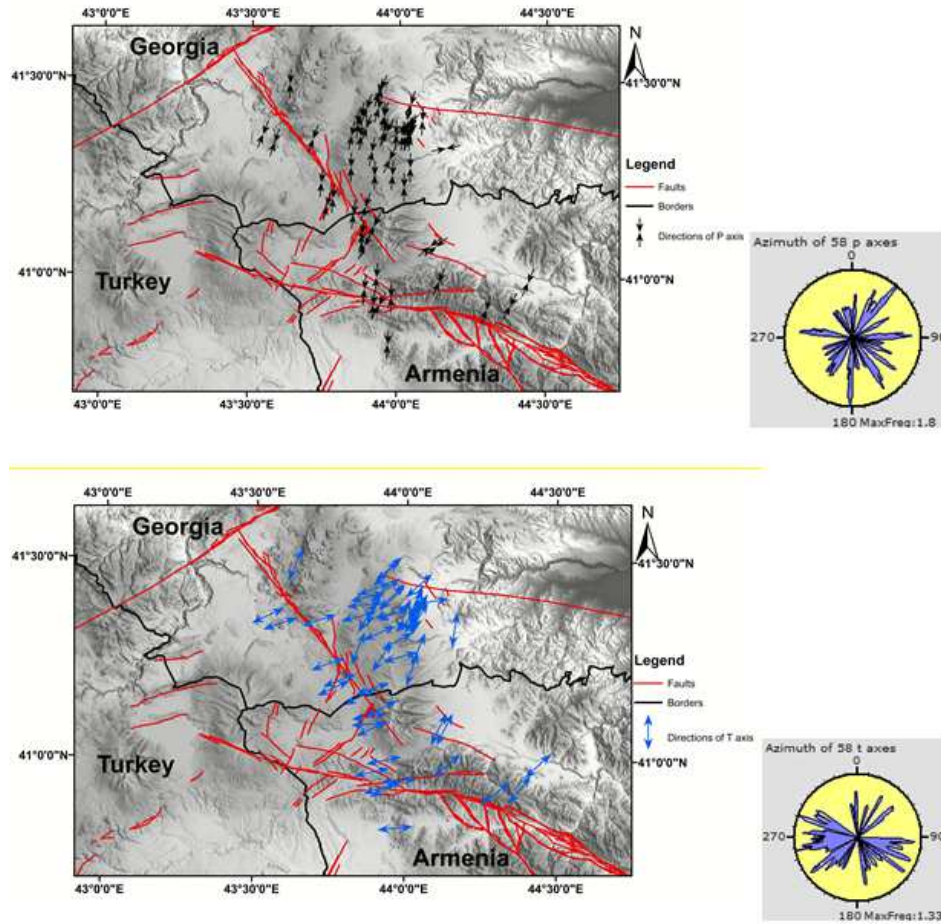
Figure 3. Focal mechanism data represented as P, T axes. Arrows indicate the tectonic regime. Inset figures show the rose diagrams of P and T axes orientations.

The focal mechanism orientations are shown by three stress axes, P, B, and T (AZ, Pl.), that are perpendicular to one another. The P- and T-axes orientations are classified according to the tectonic regime assignment proposed by Zoback, using the plunges of these axes (Zoback et al., 1980). Kinematic Compression (P) and Dilatation (T) axes directions, represented in (fig.3), indicate dominant sub-meridian directions for P axes, and sub-horizontal directions for T axes. According to the orientations of the P- and T-axes, the region experiences NE-SW compression, and NW-SE tension.

Focal mechanisms of earthquakes are the primary data used for investigating the regional tectonic stress field. Therefore, to evaluate the orientation of the stress responsible for the earthquake events, a fault-slip data inversion was performed using nodal planes and slip vectors determined from the focal mechanism solutions.

In order to analyze the stress variations throughout the region, stress tensor calculation are performed for three subgroups, which are defined based on location (fig.4; a,b,c).
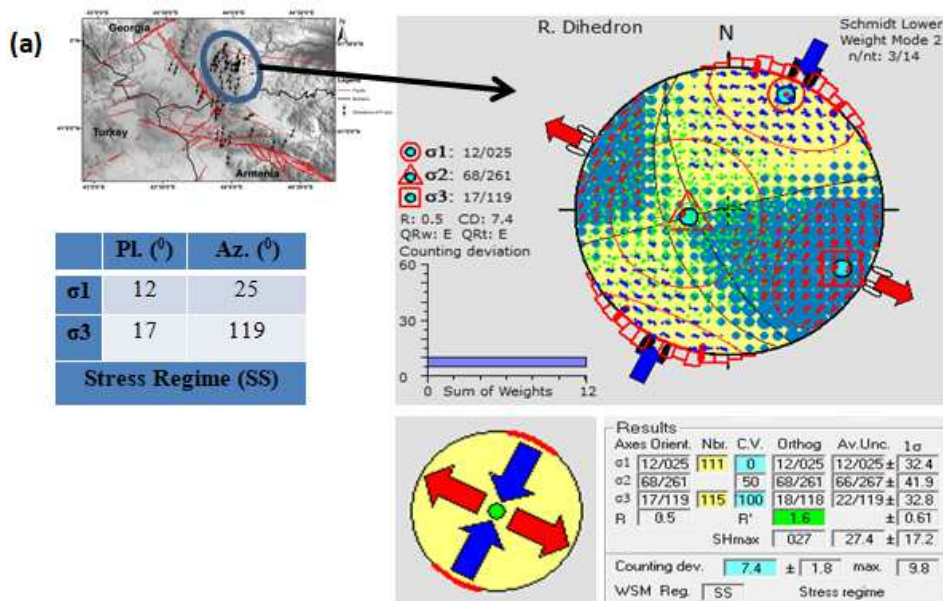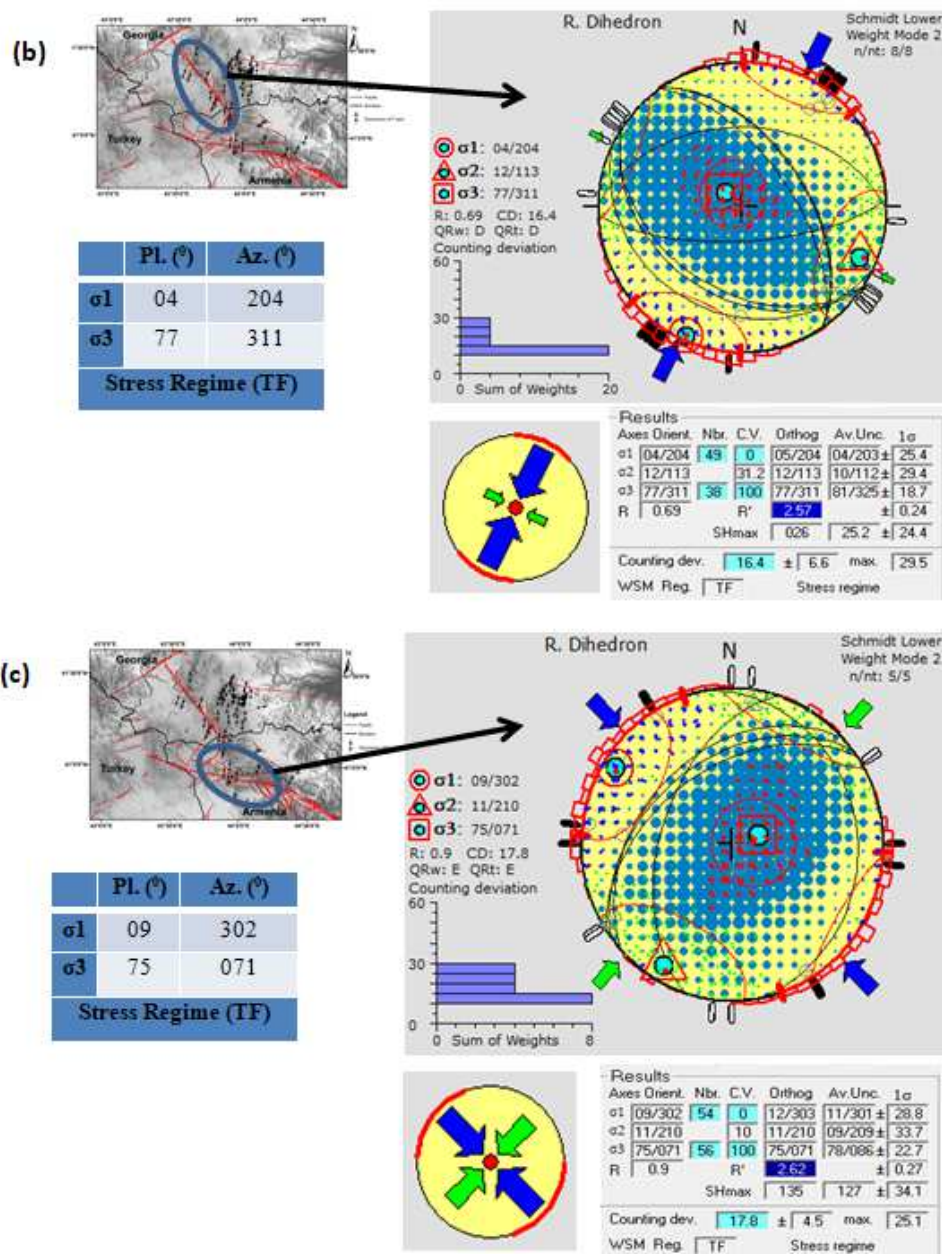
Figure 4. Stress Regimes determined for the three subgroups in the study area.

The first subgroup includes the eastern part of the Javakheti Highland. Here, a strike-slip tectonic regime is observed in the territory of Javakheti Ridge area. This subgroup has the greatest number of earthquakes characterized by strike-slip and normal faulting tectonic movement (σ1 (NE-SW), σ3 (NW–SE)) consistent with the strike-slip regime of the region (fig.4a).

The northwestern part of the study area has mainly thrust fault types of focal mechanisms, which are related to the N-S-trending parallel faults. The maximum principal stress orientations are found as ($\sigma 1$ (NE-SW), $\sigma 3$ (NW–SE)), consistent with the thrust regime of the region (fig.4b).

The third subgroup includes earthquakes located in the southern part of the study area. These events, distributed along the north-western segment of the Pambak-Sevan-Syunik active fault, are mostly of the thrust focal mechanism type movement ($\sigma 1$ (NW-SE), $\sigma 3$ (NE –SW)), consistent with the thrust regime of the region (fig.4c).

Thus, a strike-slip stress regime is observed in the eastern part of the Javakheti Highland, which is characterized by NE–SW compressional and NW–SE dilatational zones. In the study area's northwestern part, which includes the Javakheti fault zone, a thrust stress regime with a radial compressional field is observed. It coincides with a fault kinematics of this area. As for the southern part of the study area, a thrust stress regime with a radial compressional field is also observed, which is characteristic of the local kinematic features.

CONCLUSIONS

- Analysis of the distribution of focal mechanisms demonstrates the present-day tectonic activity in the study area. The solutions of the different mechanisms vary between strike-slip, thrust, and normal, but are mainly thrust. Normal faults with minor strike-slip components have fault planes trending in the NE-SW direction. The events characterized by thrust fault mechanisms are related to the zone of active faulting within the study area, trending NE-SW, and the strike slip (SS) faults primarily trend in the N-S direction.
- The events characterized by strike-slip faulting mechanisms largely occurred in the north-eastern part of the study area, along both sides of the Javakheti Ridge, where there are supposed faults. Note that the events with normal faulting mechanisms are concentrated within the Javakheti Ridge area. This indicates that strike-slip mechanisms can be linked to the supposed faulting activity, while normal faulting mechanisms can be linked to the volcanic activity in the Javakheti Ridge area.
- The kinematic Compression (P) and Dilatation (T) axes of fault planes have been determined to be dominant sub-meridian directions for P axes, and sub-horizontal directions for T axes. According to the orientations of P- and T-axes, the region experiences NE-SW compression, and NW-SE tension.
- Stress regimes were determined for the Javakheti Volcanic Highland. The northeastern part of the study area is characterized as a strike-slip stress regime ($\sigma 1$- NE-SW; $\sigma 3$-NW –SE). The northwestern part of the study area, which includes the Javakheti fault zone, a thrust stress

regime with a radial compressional field is observed (σ1-NE-SW; σ3-NW–SE). It coincides with a fault kinematics of this area. The southern part of the study area, a thrust stress regime with a radial compressional field is also observed (σ1-NW-SE; σ3-NE –SW), which is characteristic of the local kinematic features.

The parameters of the earthquakes focal mechanism solutions are presented in the table below

N₀	Date	Time	Lat. N (°)	Long. E (°)	M_L	Depth (km)	Strike (°)	Dip (°)	Rake (°)	P Az. (°)	P Pl. (°)	T Az. (°)	T Pl (°)	SH Max Azim	SH Min Azim	Regime Code	Regime Index
1	16.12.2005	04:02:28	41.16	43.85	4.3	12	270.8	43.6	47.99	209	08	104	61	26	116	2.5	TF
2	24.05.2006	03:17:19	41.08	44.11	3.7	08	107	77	-116	347	51	201	27	140	50	0.5	NF
3	28.12.2006	22:52:19	41.28	43.84	3.6	12	36	75	18	168	01	259	23	168	78	1.5	SS
4	24.07.2007	19:31:23	41.24	43.74	4.1	05	326	54	113	040	06	292	70	38	128	2.5	TF
5	09.07.2007	09:33:08	41.09	43.88	4.0	10	123	42	91	032	03	203	87	32	122	2.5	TF
6	18.06.2008	11:04:31	41.33	44.16	3.7	07	355	37	-100	127	79	272	09	1	91	0.5	NF
7	05.05.2010	14:58:22	41.38	43.89	3.5	11	197	60	179	058	20	157	22	62	152	1.5	SS
8	27.09.2011	08:58:53	41.36	43.99	4.4	12	156	73	164.6	023	02	113	22	23	113	1.5	SS
9	23.07.2011	02:49:24	41.36	43.54	3.6	08	34	24	65	323	22	169	65	138	48	2.5	TF
10	06.09.2011	00:35:44	41.37	44.04	3.5	16	256	88	33	026	21	126	24	21	121	1.5	SS
11	22.02.2011	01:24:37	41.36	43.87	3.5	15	40	65	20	352	05	259	31	171	81	1.5	SS
12	11.12.2011	14:26:34	41.35	43.71	3.4	12	2	64	93.9	089	19	280	71	88	178	2.5	TF
13	20.05.2012	23:07:26	41.00	43.93	3.5	18	198	51	104	278	05	164	78	97	7	2.5	NF
14	05.03.2012	11:12:50	41.11	43.88	3.4	09	124	38	82	040	07	255	81	39	129	2.5	TF
15	06.09.2013	16:35:26	41.36	43.84	3.8	10	120	34	76	040	12	255	76	38	128	2.5	TF
16	25.10.2013	23:45:01	41.44	44.04	3.5	08	62	70.7	50	180	17	289	48	6	96	2.5	NS
17	08.08.2013	06:20:27	41.28	44.04	3.5	05	137	72	164	004	01	095	23	4	94	1.5	SS
18	18.10.2013	18:57:18	40.83	43.97	3.2	10	236	49	86	329	04	112	85	149	59	2.5	TF
19	08.08.2013	06:38:38	41.23	44.02	3.2	15	136	76	167.6	002	01	093	19	2	92	1.5	SS
20	17.10.2013	15:04:46	40.95	43.98	3.3	08	233	44	83	148	01	047	85	148	58	2.5	TF
21	25.01.2013	20:56:43	40.97	43.89	3.3	12	227	40	73	149	06	030	77	148	58	2.5	TF
22	07.09.2013	00:34:49	41.39	43.86	3.0	15	358	49	93	086	04	298	85	86	176	2.5	NF
23	05.06.2013	16:12:52	41.18	43.89	3.1	15	116	27	78	035	19	232	71	33	123	2.5	TF
24	26.05.2014	10:57:44	41.08	44.13	4.0	13	100	80	-116	347	51	218	27	140	50	0.5	TF
25	09.03.2014	11:31:34	41.49	43.63	3.5	16	157	75	159	206	03	114	25	25	115	1.5	SS
26	25.08.2014	22:11:28	41.20	43.78	3.2	18	325.5	52.5	115	038	05	296	69	36	126	2.5	TF
27	08.11.2014	08:04:43	41.41	43.87	3.0	05	358	59	90	088	14	268	76	88	178	2.5	NF

28	14.04.2014	00:02:53	41.43	43.93	3.0	05	306	43	146.4	179	15	288	52	5	95	2.5	NS
29	16.03.2014	14:28:51	41.37	43.96	3.0	10	353	71	90.6	082	26	264	64	81	171	2.5	NF
30	24.03.2015	16:00:53	41.08	43.89	3.9	12	87	71	85	180	26	350	64	3	93	2.5	TF
31	25.05.2015	23:49:04	41.30	43.97	3.6	05	357	71	75	099	25	245	61	107	17	2.5	TF
32	08.01.2015	21:39:42	41.18	43.76	3.5	05	325	61.8	113.4	039	14	278	65	34	124	2.5	TF
33	18.07.2015	17:14:17	41.26	43.92	3.3	09	155	68	26	285	01	015	33	105	15	1.5	SS
34	27.10.2015	16:18:26	41.41	43.95	3.2	12	196	57	36	141	02	049	48	140	50	2.5	NS
35	19.04.2015	03:41:47	40.92	44.30	3.0	12	165	38	35	112	18	356	54	105	15	2.5	NF
36	12.07.2016	10:14:03	41.37	44.04	4.8	18	350.9	89.2	-161	217	13	125	12	36	126	1.5	SS
37	21.07.2016	15:17:45	41.36	44.01	4.3	10	173	69	149	226	05	132	37	44	134	1.5	SS
38	19.10.2016	03:17:56	41.36	44.04	3.7	12	172	62	18	125	08	030	32	123	33	1.5	SS
39	17.10.2016	08:11:01	41.39	44.03	3.7	20	198	74	-55	146	49	262	21	164	74	0.5	TF
40	15.08.2016	17:41:21	41.13	43.92	3.6	10	106	20	72	030	26	225	63	25	115	2.5	TF
41	13.07.2016	15:34:43	41.34	43.58	3.6	10	10	26	89	281	19	102	71	101	11	2.5	TF
42	12.07.2016	10:16:01	41.36	44.03	3.5	14	11	89	-164	236	12	144	11	55	145	1.5	SS
43	13.07.2016	03:17:16	41.38	44.04	3.4	15	161	55	170	024	18	125	30	29	119	1.5	SS
44	05.01.2016	12:24:09	41.43	43.89	3.4	10	170	25	83	085	20	275	70	84	174	2.5	NF
45	24.03.2016	03:54:09	40.93	44.38	3.2	10	252	39	9	215	28	099	38	24	114	2.5	TF
46	02.03.2016	03:43:55	41.41	43.95	3.2	08	97	71.7	137.4	155	14	052	42	150	60	1.5	NS
47	16.03.2106	21:02:10	40.99	44.44	3.1	10	147	76.4	124.7	211	23	093	47	22	112	2.5	TF
48	04.08.2016	11:26:40	41.36	44.02	3.1	12	274	71	162	142	01	232	26	142	52	1.5	SS
49	04.08.2016	21:07:03	41.40	44.03	3.0	10	14	71	21	145	03	236	24	146	56	1.5	SS
50	24.03.2017	01:24:01	41.47	43.93	3.7	05	315	47	156	183	16	289	44	9	99	2.5	TF
51	24.03.2017	01:30:35	41.48	43.94	3.0	05	321	39	156	187	21	302	47	15	105	2.5	TF
52	18.04.2017	06:49:34	40.99	44.14	3.1	19	314	35	153	181	23	302	50	10	100	2.5	TF
53	18.04.2017	08:28:59	41.40	44.08	3.0	09	348	43	101	250	03	358	82	70	160	2.5	NF
54	09.05.2017	06:32:43	41.32	43.91	3.1	08	1	58	64	110	10	223	66	113	23	2.5	NF
55	09.05.2017	11:07:24	41.26	43.98	3.6	10	20.8	51	69.9	125	04	230	74	126	36	2.5	NF
56	04.07.2017	06:21:11	40.93	43.94	3.7	05	350	18	71	275	28	109	62	90	0	2.5	TF
57	15.08.2017	05:12:01	40.93	43.92	3.2	08	349	42	65	276	06	168	73	94	4	2.5	TF
58	11.01.2017	19:29:01	41.37	43.95	3.2	12	11.6	59.5	95.9	098	15	298	74	96	006	2.5	NF

REFERENCE

Balassanian S., T. Ashirov, T. Chelidze A., Gassanov N., Kondorskaya G., Molchan…and M. Stucchi, 1999, "Seismic hazard assessment for the Caucasus test area", *Ann. Geofis.*, *42*(6), p.1139-1164.

Davtyan V. 2007, **"**Active faults of Armenia: slip rate estimation by GPS, paleo seismological and morph structural data". PhD Thesis, Montpellier II University, France.

Delvaux D., Moeys R., Stapel G. **et al.** 1997b, "Paleo stress reconstructions and geodynamics of the Baikal region, Central Asia. Part II: Cenozoic tectonic stress and fault kinematics". Tectonophysics, 282(1-4), p.1-38.

Delvaux D. and Sperner B. 2003, "New aspects of tectonic stress inversion with reference to the TENSOR program" NIEUWLAND, New Insights into Structural Interpretation and Modelling, Geological Society, London, Special Publications, 212, p.75-100.

Duff R. E. and Peterson F. I. 1980, Shock precursor observations, Precursor transition in dynamical systems undergoing period doubling, J. App. Phys., 51, 7; p.3957–3959.

Froehlich C. 1992, "Tringle diagrams ternary graphs to display similarity and diversity of earthquake focal mechanisms" Phys Earth Planet Inter, 75; p.193-198

Karakhanian A., Avagyan A., Avanessyan M., Elashvili M., Godoladze T., Javakhishvili Z., Korzhenkov A., Philip S., and Vergino E. 2012, Armenia-to-Georgia trans-boundary fault: An example of international cooperation in the Caucasus: San Francisco, California, American Geophysical Union, Fall Meeting supplement, abstract S43J-02.

Karakhanyan A., Vernant P., Doerfl inger E., Avagyan A., Philip H., Aslanyan R., Champollion C., Arakelyan S., Collard P., Baghdasaryan H., Peyret M., Davtyan V., Calais E. and Masson F. 2013, GPS constraints on continental deformation in the Armenian region and Lesser Caucasus: Tectonophysics, v. 592, doi:10.1016/j.tecto. 02.002; p. 39–45.

Karakhanyan A., Arakelyan A., Avagyan A. and Sadoyan T. 2016, "Aspects of the seismo-tectonics of Armenia: New data and reanalysis", in Sorkhabi, R., ed., Tectonic Evolution, Collision, and Seismicity of Southwest Asia: In Honor of Manuel Berberian's Forty-Five Years of Research Contributions: Geological Society of America Special Paper 525;

Lander A.V., 2004, The FA2002 program system to determine the focal mechanisms of earthquakes in Kamchatka, the Commander Islands and the Northern Kuriles. Report KEMSD GS RAS, Petropavlovsk-Kamchatsky, 250 pages.

Lebedev V.A., Chernyshev I.V., Dudauri O.Z., Arakelyants M.M., Bairova, E.D., Gol'tsman Yu. V., Chugaev A.V., Vashakidze G.T. 2003, "The Samsari Volcanic Center as an Example of Recent Voclanism in the Lesser Caucasus: K-Ar Geochronological and Sr-Nd Isotopic data". Dokl. Earth Sci. 393A, p.1323-1328.

Nomade S., Scao V., Guillou H., Messager E., Mgeladze A., Voinchet P., Renne P.R., Courtin-Nomade A., Bardintzeff J.M., Ferring R., Lordkipanidze D. 2015, "New-40Ar/39Ar, unspiked K/Ar and geochemical constraints on the Pleistocene magmatism of the Samtskhe-Javakheti highlands (Republic of Georgia)", Quaternary International, p.1-15.

Philip H., Avagyan A., Karakhanyan A., Ritz J.-F. and Rebai S., 2001, "Slip rates and recurrence intervals of strong earthquakes along the Pambak- Sevan-Sunik Fault (Armenia)": Tectonophysics, v. 343, no. 3–4, p.205–232.

Reilinger R., McClusky S., Vernant P., Lawrence S., Ergintav S., Cakmak R., Ozener H., Kadirov F., Guliev I., Stepanyan R., Nadariya M., Hahubia G., Mahmoud S., Sakr K., Abdullah ArRajehi, Paradissis D., Al- Aydrus A., Prilepin M., Guseva T., Evren E., Dmitrotsa A., Filikov S.V., Gomez F., Al-Ghazzi R. and Karam G. 2006, "GPS constraints on continental deformation in the Africa-Arabia-Eurasia continental collision zone and implications for the dynamics of plate interactions": Journal of Geophysical Research–Solid Earth, v. 111, no. B5, p.1–26, doi:10.1029/2005JB004051

Zoback M.L., Zoback M.D. 1980, State of stress in the Conterminous United States. J. Geophys. Res., 85,; p. 6113-6156.

Введенская А.В., Балакина Л.М. 1960, Методика и результаты определения напряжений, действующих в очагах землетрясений Прибайкалья и Монголии // Бюлл. Совета по сейсмологии. № 10. с.73-84.

Reviewer A.Araqelyan

ՋԱՎԱԽՔԻ ՀՐԱԲԽԱՅԻՆ ԲԱՐՁՐԱՎԱՆԴԱԿԻ ԼԱՐՎԱԾԱՅԻՆ ԴԱՇՏԻ ԱՌԱՆՁՆԱՀԱՏԿՈՒԹՅՈՒՆՆԵՐԸ ԵՐԿՐԱՇԱՐԺԵՐԻ ՖՈԿԱԼ ՄԵԽԱՆԻԶՄՆԵՐԻ ՀԱՇՎԱՐԿԻ ԿԻՐԱՌՄԱՄԲ 2005-2017ԹԹ. ԺԱՄԱՆԱԿԱՇՐՋԱՆԻ ՀԱՄԱՐ

Է.Է.Սահակյան

Ամփոփում

Աշխատանքում իրականացվել է Ջավախքի հրաբխային բարձրա-վանդակում 2005-2017 թթ☐ ընթացքում գրանցված երկրաշարժերի ֆո-կալ մեխանիզմների հաշվարկ: Օգտագործվել են Հայաստանի, Վրաս-տանի, ինչպես նաև հարակից մյուս սեյսմիկ կայանների կողմից գրանցված երկրաշարժերի թվային ալիքային պատկերները: Ֆոկալ մեխանիզմները հաշվարկվել են P ալիքի առաջին մուտքի նշանի մե-թոդի կիրառմամբ: Լուծումները տրվել են P ալիքի բևեռացման, սեյս-միկ կայանի նկատմամբ ազիմուտային անկյան, ինչպես նաև ալիքի անկման անկյան տվյալների հիման վրա: Այն երկրաշարժերը, որոնց համար հաշվարկվել են ֆոկալ մեխանիզմները, իրականացվել է նաև էպիկենտրոնների և հիպոկենտրոնների վերահաշվարկ (re-location):

Ուսումնասիրվող գոտու լարվածային ռեժիմի գնահատման հա-մար օգտագործվել են վերոնշյալ երկրաշարժերի խզման հարթություն-ների լուծումները:

Ջավախքի բարձրավանդակում երկրաշարժերը բնութագրվում են շարժման տարբեր տիպի կինեմատիկաներով (կողաշարժային, վեր-նետքային, վարնետքային), բայց նշված ժամանակահատվածի համար գերակշռում են վերնետքային տիպի մեխանիզմով երկրաշարժերը: Լարվածային ռեժիմը գոտու տարբեր հատվածներում հաշվարկվել է կողաշարժային և վերնետքային տիպի:

ОСОБЕННОСТИ ПОЛЯ НАПРЯЖЕНИЙ ДЖАВАХЕТСКОГО ВУЛКАНИЧЕСКОГО НАГОРЬЯ, ОПРЕДЕЛЕННЫЕ ПО ФОКАЛЬНЫМ МЕХАНИЗМАМ ЗЕМЛЕТРЯСЕНИЙ ЗА ПЕРИОД 2005-2017 ГГ.

Э.Э. Саакян

Резюме

Джавахетское вулканическое нагорье, расположенное на Центральном Кавказе, является частью зоны континентальной коллизии Аравии и Ев-разии. Эта область характеризуется повышенной сейсмической актив-ностью и вулканизмом, где распределение землетрясений рассеянное.

В данном исследовании мы изучаем механизмы очагов землетрясений с использованием цифровых волновых данных, зарегистрированных сейсмическими станциями армянской, грузинской и смежных с ними сейсмических сетей. Мы строим фокальные механизмы для группы землетрясений, произошедших в период 2005–2017гг, с большим уровнем надежности, на основе полярности первого вступления Р-волны. Для получения первоначальных решений фокальных механизмов использовались азимут, угол наклона и полярности Р-фазы. Было проведено также переопределение мест для выбранных сейсмических событий за данный временной период.

Решения плоскости разлома для зарегистрированных землетрясений применялись для определения реальной геометрии разломов, типа разломообразования и режима напряжений на исследованной территории.

Мы объединили все надежно задокументированные фокальные механизмы по десяткам землетрясений с целью изучения текущего состояния напряжений в коре в пределах Джавахетского вулканического нагорья. Землетрясения Джавахетского нагорья характеризуются различной кинематикой (сдвиги, взбросы, сбросы), но для указанного промежутка времени преобладают землетрясения с механизмами взбросового типа. В различных участках зоны существуют разные режимы напряжений – сдвиговые и взбросовые.